

## Metal-Organic Frameworks Based on Trigonal Prismatic Building Blocks and the New “acs” Topology

Andrea C. Sudik, Adrien P. Côté, and Omar M. Yaghi\*

Materials Design and Discovery Group, Department of Chemistry, University of Michigan, 930 North University, Ann Arbor, Michigan 48109-1055

Received January 15, 2005

Cationic and mixed-valent forms of  $\text{Fe}_3\text{O}(\text{CO}_2)_6$  trigonal prismatic clusters have been linked by ditopic links, namely, 1,4-benzenedicarboxylate (1,4-BDC) and 1,3-benzenedicarboxylate (1,3-BDC), to produce two 3-periodic metal–organic frameworks (MOFs),  $[\text{Fe}_3\text{O}(1,4\text{-BDC})_3(\text{DMF})_3][\text{FeCl}_4]\cdot(\text{DMF})_3$  (MOF-235) and  $\text{Fe}_3\text{O}(1,3\text{-BDC})_3(\text{py})_3\cdot(\text{py})_{0.5}(\text{H}_2\text{O})_{1.5}$  (MOF-236) (DMF = *N,N*-dimethylformamide, py = pyridine), respectively. These MOFs exemplify a new, high-symmetry topology termed **acs** which we identify here as the default arrangement for linking trigonal prisms together.

It is our thesis that for a given molecular shape only a few simple high-symmetry nets are of general importance, and they are likely to form when metal ions are copolymerized with organic links.<sup>1</sup> We call these “default nets” in that they are the nets that form in the absence of designing into the assembly complexity such as bent linkers, structure directing agents (templates), sterically constraining ligands, or counterions.<sup>2</sup> Thus, identification of the default structures for a given combination of building blocks is essential for developing a road map toward designing materials with predetermined properties. At present many examples of metal–organic frameworks (MOFs) have been reported for the default nets expected from the assembly of tetrahedral, square, triangular, and octahedral building blocks.<sup>3</sup> However, 3-periodic MOF structures based on the assembly of trigonal prismatic building units remain largely unexplored.<sup>4,5</sup> Here, we report the synthesis and structure of two MOFs constructed from oxo-centered trinuclear iron clusters and benzenedicarboxylate links to give structures whose underlying

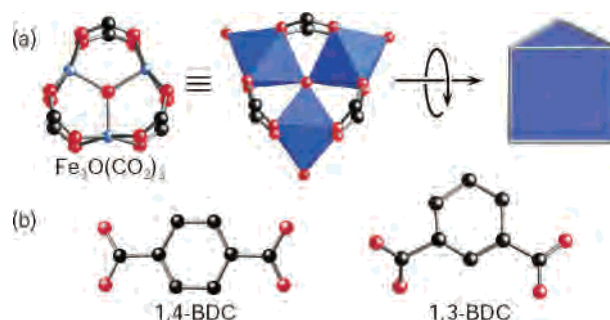


**Figure 1.** Inorganic and organic building units used to assemble MOF-235 and MOF-236: (a) oxygen-centered iron-carboxylate trimer ( $\text{Fe}_3\text{O}(\text{CO}_2)_6$ , Fe, blue; O, red; C, gray) shown in ball-and-stick and polyhedral representations of trigonal prismatic geometry (blue) and (b) ditopic links, 1,4-benzenedicarboxylate (1,4-BDC) or 1,3-benzenedicarboxylate (1,3-BDC).

ing topology is the one we assign as the default net for the assembly of trigonal prismatic building blocks.

The carboxylate carbon atoms in the  $\text{Fe}_3\text{O}(\text{CO}_2)_6$ -type cluster serve as the points-of-extension that define the vertexes of a trigonal prismatic secondary building unit (SBU) (Figure 1a). In this study, such an SBU has been linked by two ditopic links: 1,4-benzenedicarboxylate (1,4-BDC) and 1,3-benzenedicarboxylate (1,3-BDC) (Figure 1b) to give  $[\text{Fe}_3\text{O}(1,4\text{-BDC})_3(\text{DMF})_3][\text{FeCl}_4]\cdot(\text{DMF})_3$  (MOF-235) and  $\text{Fe}_3\text{O}(1,3\text{-BDC})_3(\text{py})_3\cdot(\text{py})_{0.5}(\text{H}_2\text{O})_{1.5}$  (MOF-236); (DMF = *N,N*-dimethylformamide, py = pyridine). These isostructural MOFs are examples of the **acs** net; a hexagonal net of aligned, corner-sharing trigonal prisms to be discussed below.

These MOFs were obtained as pure phase materials by heating equimolar amounts of dicarboxylic acid link (1,4-H<sub>2</sub>BDC for MOF-235 or 1,3-H<sub>2</sub>BDC for MOF-236) and iron salt ( $\text{FeCl}_3\cdot(\text{H}_2\text{O})_6$  for MOF-235 or  $\text{FeBr}_2$  for MOF-236) in

\* Author to whom correspondence should be addressed. E-mail: oyaghi@umich.edu.

- (1) (a) O’Keeffe, M.; Eddaoudi, M.; Li, H.; Reineke, T. M.; Yaghi, O. M. *J. Solid State Chem.* **2000**, *152*, 3. (b) Kim, J.; Chen, B.; Reineke, T. M.; Li, H.; Eddaoudi, M.; Moler, D. B.; O’Keeffe, M.; Yaghi, O. M. *J. Am. Chem. Soc.* **2001**, *123*, 8239. (c) Yaghi, O. M.; O’Keeffe, M.; Ockwig, N. W.; Chae, H. K.; Eddaoudi, M.; Kim, J. *Nature* **2003**, *423*, 705.
- (2) (a) Carlucci, L.; Ciani, G.; Proserpio, D. M.; Rizzato, S. *Chem. Commun.* **2001**, 1198. (b) Kitazawa, T.; Kikuyama, T.; Takeda, M.; Iwamoto, T. *J. Chem. Soc., Dalton Trans.* **1995**, 22, 3715. (c) Li, H.; Laine, A.; O’Keeffe, M.; Yaghi, O. M. *Science* **1999**, *283*, 1145. (d) Keller, S. W. *Angew. Chem., Int. Ed.* **1997**, *36*, 247.

- (3) (a) Batten, S. R.; Robson, R. *Angew. Chem. Int. Ed.* **1998**, *37*, 1460. (b) Kitagawa, S.; Kitaura, R.; Noro, S.-I. *Angew. Chem., Int. Ed.* **2004**, *43*, 2334. (c) Lu, J.; Mondal, A.; Moulton, B.; Zaworotko, M. J. *Angew. Chem., Int. Ed.* **2001**, *40*, 2113. (d) Carlucci, L.; Ciani, G.; Proserpio, D. M.; Sironi, A. *J. Am. Chem. Soc.* **1995**, *117*, 12861. (e) Klein, C.; Graf, E.; Hosseini, M. W.; Cian, A. D. *New J. Chem.* **2001**, *25*, 207. (f) Eddaoudi, M.; Moler, D. B.; Li, H.; Chen, B.; Reineke, T. M.; O’Keeffe, M.; Yaghi, O. M. *Acc. Chem. Res.* **2001**, *34*, 319.
- (4) (a) Yang, G.; Raptis, R. G. *Chem. Commun.* **2004**, 2058. (b) Serre, C.; Millange, F.; Surlé, S.; Férey, G. *Angew. Chem., Int. Ed.* **2004**, *43*, 6290.
- (5) Barthelet, K.; Riou, R.; Férey, G. *Chem. Commun.* **2002**, 1492.

a DMF (MOF-235) or pyridine (MOF-236) and ethanol solvent mixture.<sup>6</sup> Orange MOF-235 or green MOF-236 hexagonal single crystals were produced in 42% (MOF-235) or 34% (MOF-236) yield and analyzed by single-crystal X-ray diffraction studies, elemental analysis, magnetic measurements, FT-IR spectroscopy, and TGA.<sup>6,7</sup> The bulk phase purity of each sample was confirmed by comparison of the observed and simulated PXRD patterns.<sup>6</sup>

In MOF-235, each iron atom is trivalent, yielding an overall cationic (+1 per formula unit) framework. This charge is balanced by  $\text{FeCl}_4^-$  counterions whose identity was confirmed by single-crystal X-ray data and far FT-IR measurements,<sup>8</sup> these counterions are located in the hexagonal pores of the structure (Figure 2a). In MOF-236, each iron trimer is mixed-valent to yield an overall neutral framework (Figure 2b).

The magnetic susceptibilities for both MOFs were measured to determine if the magnetic behavior of the iron oxide clusters is consistent with that of their unlinked molecular

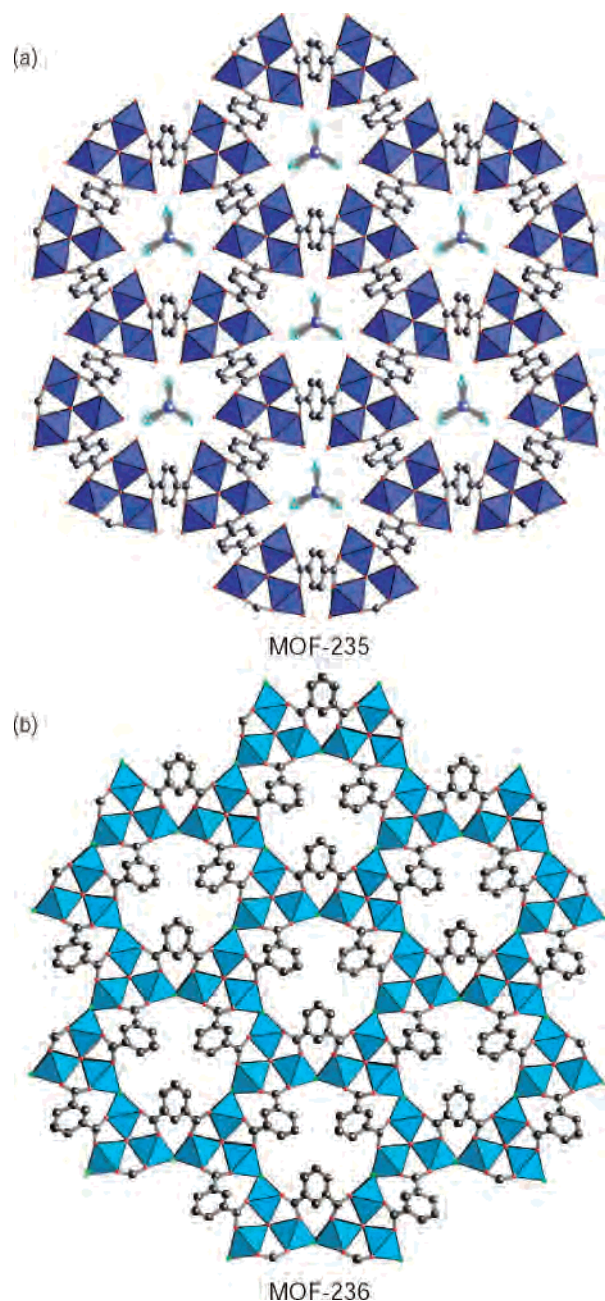


**Figure 2.** Single-crystal X-ray structures of (a) MOF-235 (Fe, blue; O, red; Cl, teal; C, gray) and (b) MOF-236 (Fe, light blue; O, red; C, gray; N, green) composed of oxo-centered iron trimers and benzenedicarboxylate links (views down  $z$ -axis). Axial coordinating ligands and hydrogen atoms have been omitted for clarity.

(6) MOF-235: Equimolar amounts of  $\text{FeCl}_3 \cdot (\text{H}_2\text{O})_6$  (0.2 g, 1.23 mmol) and 1,4- $\text{H}_2\text{BDC}$  (0.205 g, 1.23 mmol) were dissolved in 60 mL of DMF. Pyrex tubes (i.d.  $\times$  o.d. =  $8 \times 10$  mm<sup>2</sup>, 140 mm length) containing 2 mL of the reaction solution and 2 mL of ethanol were flash frozen (liquid  $\text{N}_2$ ), evacuated, flame sealed, and placed in an 85 °C oven for 24 h. The orange octahedral crystals of MOF-235 (42% yield based on 1,4- $\text{H}_2\text{BDC}$ ) were washed with a DMF/ethanol mixture. Anal. Calcd (%) for  $[\text{Fe}_3\text{O}(1,4\text{-BDC})_3(\text{DMF})_3][\text{FeCl}_4] \cdot (\text{DMF})_3$ : C, 38.45; H, 4.15; N, 6.40. Found: C, 38.34; H, 4.63; N, 6.39. FT-IR (KBr, 3500–400  $\text{cm}^{-1}$ ): 3440 (m), 2931 (w), 1663 (s), 1597 (vs), 1505 (m), 1439 (s), 1398 (vs), 1016 (m), 823 (m), 750 (s), 554 (s). Far IR: 528 (s), 419 (m), 386 (m), 336 (s). PXRD ( $\text{\AA}$ ,  $I/I_0$ ): 9.29 (100), 6.99 (24), 6.28 (14), 5.31 (18), 4.68 (76), 4.02 (37), 3.38 (15), 3.13 (17). TGA: 30–50 °C, –4.34% obsd (excess solvent); 50–75 °C, –17.81% obsd (–16.7% calcd for loss of 3 free DMF); 75–350 °C, –25.80% obsd (–20.1% calcd for loss of 3 ligated DMF); 350 °C, decomp of MOF-235. MOF-236: Equimolar amounts of  $\text{FeBr}_2$  (0.1 g, 0.46 mmol) and 1,3- $\text{H}_2\text{BDC}$  (0.08 g, 0.46 mmol) were dissolved in 40 mL of pyridine. Shell vials (4 mL capacity) containing 2.1 mL of the reaction solution and 0.9 mL of absolute ethanol were prepared, capped, and placed in a 100 °C oven for 24 h. The octahedral green crystals of MOF-236 (34% yield based on 1,3- $\text{H}_2\text{BDC}$ ) were washed with a pyridine/ethanol mixture. Anal. Calcd (%) for  $[\text{Fe}_3\text{O}(1,3\text{-BDC})_3(\text{py})_3] \cdot (\text{py})_{0.5}(\text{H}_2\text{O})_{1.5}$ : C, 50.87; H, 3.34; N, 5.00. Found: C, 50.60; H, 3.28; N, 5.08. FT-IR (KBr, 3500–400  $\text{cm}^{-1}$ ): 3435 (m), 3073 (w), 2931 (w), 1622 (vs), 1601 (m), 1581 (m), 1482 (w), 1449 (m), 1398 (vs), 1220 (w), 1042 (w), 750 (m), 708 (s), 700 (s), 468 (s). PXRD ( $\text{\AA}$ ,  $I/I_0$ ): 11.36 (32), 8.99 (100), 7.34 (30), 6.17 (25), 4.89 (51), 4.30 (23), 4.13 (12), 3.78 (12), 3.71 (16), 3.23 (11), 2.79 (8). TGA: 30–350 °C, –26.30% obsd (multistep loss, –31.00% calcd for loss of 0.5 free py, 1.5 free  $\text{H}_2\text{O}$ , and 3 ligated py); 350 °C, decomp of MOF-236.

(7) For both compounds the optimal crystals available for analysis were small and weakly scattering. The best resolution in the data obtained was 0.8  $\text{\AA}$ , which is reflected in the large residuals for modeled structures. Full details on data handling and structure solution are given in the Supporting Information. Crystal data (Bruker SMART APEX CCD, graphite-monochromated Mo  $\text{K}\alpha$  radiation). MOF-235 ( $\text{C}_{33}\text{H}_{15}\text{-Fe}_4\text{Cl}_4\text{N}_5\text{O}_{17}$ ):  $T = 153(2)$  K, hexagonal, space group  $P62c$  (No. 190),  $a = 12.531(3)$   $\text{\AA}$ ,  $c = 18.476(11)$   $\text{\AA}$ ,  $V = 2512.6(17)$   $\text{\AA}^3$ ,  $Z = 2$ ,  $\rho_{\text{calcd}} = 1.442$   $\text{g}\cdot\text{cm}^{-3}$ ,  $\mu = 1.407$   $\text{mm}^{-1}$ , 11327 measured reflections, 1543 unique reflections ( $R_{\text{int}} = 0.1441$ ), 116 parameters, 1 restraint,  $R_1 = 0.1044$  for 1543 observed reflections ( $I > 2.0\sigma(I)$ ),  $R_w(\text{all data}) = 0.2550$ ,  $S = 1.260$ ,  $\Delta\rho = 1.429$   $\text{e}\text{\AA}^{-3}$ . MOF-236 ( $\text{C}_{37}\text{H}_{18}\text{Fe}_3\text{N}_{3.5}\text{O}_{16}$ ):  $T = 153(2)$  K, hexagonal, space group  $P62c$  (No. 190),  $a = 13.017(4)$   $\text{\AA}$ ,  $c = 14.896(8)$   $\text{\AA}$ ,  $V = 2185.9(15)$   $\text{\AA}^3$ ,  $Z = 2$ ,  $\rho_{\text{calcd}} = 1.478$   $\text{g}\cdot\text{cm}^{-3}$ ,  $\mu = 1.057$   $\text{mm}^{-1}$ , 6065 measured reflections, 946 unique reflections ( $R_{\text{int}} = 0.2551$ ), 92 parameters, 2 restraints,  $R_1 = 0.0651$  for 543 observed reflections ( $I > 2.0\sigma(I)$ ),  $R_w(\text{all data}) = 0.1193$ ,  $S = 1.004$ ,  $\Delta\rho = 1.478$   $\text{e}\text{\AA}^{-3}$ .

(8) Fe–Cl bond stretches observed in far-IR at 385.6 and 335.7  $\text{cm}^{-1}$  are assigned to  $\nu_3$  and  $\nu_1$  stretching modes, respectively. Sreekanth, A.; Kurup, M. R. P. *Polyhedron* **2004**, *23*, 969.

counterparts. Experiments were conducted in the temperature range of 5–300 K at a constant magnetic field (5 kG). The  $\mu_{\text{eff}}$  values at 300 K per iron, 3.23  $\mu_{\text{B}}$  (MOF-235) and 3.11  $\mu_{\text{B}}$  (MOF-236), are considerably smaller than the calculated spin-only values. Both compounds exhibit a gradual decrease in magnetic moment to 1.95  $\mu_{\text{B}}$  (MOF-235) and 1.02  $\mu_{\text{B}}$  (MOF-236) at 5 K indicating antiferromagnetic coupling interactions between iron centers. In MOF-235, the low-temperature data do not extrapolate toward zero; whereas in MOF-236 an abrupt decrease in the  $\mu_{\text{eff}}$  value is observed which is typical of such mixed valent iron trimers. The room temperature values for both compounds are consistent with

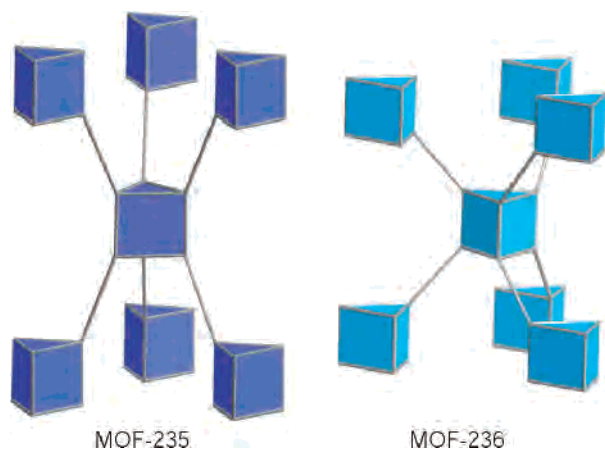


**Figure 3.** Trigonal prismatic SBUs (blue) and ditopic links (gray) are reticulated into decorated and expanded versions of the **acs** net, a hexagonal ABA array of trigonal prisms.

values previously reported for molecular  $[\text{Fe}_3\text{O}(\text{RCO}_2)_6\text{L}_3]^{+0}$  systems ( $3.0\text{--}3.9 \mu\text{B}$ ).<sup>9,10</sup> Long-range coupling is presumed to be negligible.

The crystal structures of MOF-235 and MOF-236 show that the two compounds are topologically identical. Each is built-up from corner-sharing octahedral iron trimers that are connected through linear (1,4-BDC) or bent (1,3-BDC) links as shown in Figure 2a and b, respectively. The  $\text{Fe}_3\text{O}$  plane of each trimer has  $\text{Fe}-(\mu_3\text{-O})-\text{Fe}$  angles ( $120^\circ$ ) and  $\text{Fe}-\text{Fe}$  separations of  $3.33 \text{ \AA}$  (MOF-235) and  $3.31 \text{ \AA}$  (MOF-236) that are consistent with previously reported tri- and mixed-valent  $\text{Fe}_3\text{O}$  clusters ( $120^\circ$ ,  $3.3\text{--}3.4 \text{ \AA}$ ).<sup>9</sup> This unit is linked by six separate ditopic organic links with each carboxylate bound in a bidentate fashion to adjacent iron centers. Two, 3-periodic structures are produced each having hexagonal pores whose vertexes are the central oxo anions of the  $\text{Fe}_3\text{O}$  clusters. The diameter of the primary hexagonal channel (along the  $z$ -axis) in MOF-235 is  $6.7 \text{ \AA}$ ; this becomes reduced to  $1.9 \text{ \AA}$  in MOF-236 due to the protruding phenyl rings of 1,3-BDC.<sup>11</sup>

MOF-235 and MOF-236 have a rarely observed underlying topology. By considering the points-of-extension (carboxylate C atoms) in both structures, one obtains trigonal prismatic SBUs (6-connected) that are joined by ditopic links (2-connected) as shown in Figure 3. The overall network is based on the **acs** topology, which has already been described in an earlier publication.<sup>12</sup> This topology has been observed for linking such clusters but with more flexible links than

those used here, further validating the **acs** topology as a default net.<sup>4</sup> We note that the structures of MOF-235 and MOF-236 are decorated and expanded versions of the **acs** net, where each 6-coordinate vertex is replaced by a trigonal prism (decoration) and spaced apart from each other by the 2-coordinated organic links (expansion).

Typically, link extension in MOF construction results in a uniform expansion in all three dimensions.<sup>13</sup> MOF-235 and MOF-236 demonstrate that an asymmetrical adjustment of the metrics can be achieved while maintaining the underlying topology. Here, this is realized by altering the linker geometry, resulting in a unidirectional compression along  $z$  for MOF-236. Unlike MOF-235, where the carboxylate functionalities are oriented at  $180^\circ$  to each other, in MOF-236 they are oriented at  $120^\circ$ . The closer proximity of  $\text{CO}_2$  groups of 1,3-BDC in MOF-236 yields the compressed version of MOF-235. While the hexagonal edge length between each  $\text{Fe}_3\text{O}$  vertex is only modestly affected ( $7.23(3) \text{ \AA}$  for MOF-235;  $7.06(3) \text{ \AA}$  for MOF-236), the more significant metrical modification is a contraction of the AB layer distance ( $9.24(3) \text{ \AA}$  for MOF-235;  $7.45(3) \text{ \AA}$  for MOF-236) (Figure 3).

Aside from the hexagonal **acs** topology as a default net for uninodal (all same geometry at the vertex) trigonal prismatic MOFs, only one other example exists, namely a decorated primitive cubic arrangement.<sup>5</sup> This framework is built-up from building blocks similar to those in MOF-236, specifically trigonal prismatic  $\text{V}_3\text{O}(\text{CO}_2)_6$  clusters and 1,3-BDC links to give a cubic structure. Here, the trigonal prismatic vertexes are now tilted at  $70.5^\circ$  ( $180^\circ$  in MOF-236) with respect to each other due to having water terminal ligands rather than pyridine as in MOF-236. We believe that deviation from the default **acs** net for this compound is mainly due to the character of the terminal ligands whose size may play a structure directing role. In other words, it provides more information to the trigonal prismatic SBU to fall into a structure belonging to a nondefault net.

**Acknowledgment.** We thank The National Science Foundation (DMR 0242630) and the Department of Energy (DOE) for support and Professor Michael O’Keeffe for his invaluable comments. A.P.C. thanks Science and Engineering Research Canada (NSERC) for a PDF fellowship.

**Supporting Information Available:** Complete descriptions of the X-ray single-crystal structural collection and analysis, PXRD patterns, magnetic susceptibility data, and TGA curves for MOF-235 and MOF-236 (pdf), and crystallographic information files (cif). This material is available free of charge via the Internet at <http://pubs.acs.org>.

IC050064G

- (9) Cannon, R. D.; White, R. P. *Prog. Inorg. Chem.* **1988**, *36*, 195.  
 (10) (a) Hibbs, W.; van Koningsbruggen, P. J.; Arif, A. M.; Shum, W. W.; Miller, J. S. *Inorg. Chem.* **2003**, *42*, 5645. (b) Baranwal, B. P.; Das, S. S.; Gupta, T.; Singh, A. K. *Prog. Cryst. Growth Charact. Mater.* **2002**, *45*, 147.  
 (11) Diameter measurements performed using Cerius2 and correspond to the largest sphere that could occupy the channel without contacting the van der Waals surface of the framework.  
 (12) Delgado Friedrichs, O.; O’Keeffe, M.; Yaghi, O. M. *Acta Crystallogr. A* **2003**, *59*, 22.

- (13) Eddaoudi, M.; Kim, J.; Rosi, N.; Vodak, D.; Wachter, J.; O’Keeffe, M.; Yaghi, O. M. *Science* **2002**, *295*, 469.